Elastically Driven Linker Aggregation between Two Semiflexible Polyelectrolytes

Itamar Borukhov,[1,2] Robijn F. Bruinsma,[2,3] William M. Gelbart,[1] and Andrea J. Liu[1]

[1]*Department of Chemistry and Biochemistry, University of California at Los Angeles, Los Angeles, California 90095*
[2]*Department of Physics, University of California at Los Angeles, Los Angeles, California 90095*
[3]*Instituut-Lorentz for Theoretical Physics, Universiteit Leiden, Postbus 9506, 2300 RA Leiden, The Netherlands*

(Received 26 September 2000)

The behavior of mobile linkers connecting two semiflexible charged polymers, such as polyvalent counterions connecting DNA or F-actin chains, is studied theoretically. The chain bending rigidity induces an effective repulsion between linkers at large distances while the interchain electrostatic repulsion leads to an effective short-range interlinker attraction. We find a rounded phase transition from a dilute linker gas where the chains form large loops between linkers to a dense disordered linker fluid connecting parallel chains. The onset of chain pairing occurs within the rounded transition.

DOI: 10.1103/PhysRevLett.86.2182 PACS numbers: 87.15.–v, 41.20.Cv, 61.20.Qg, 61.25.Hq

Highly charged chains of the same sign can be linked together by mobile polyvalent ions of the opposite sign (polyvalent counterions). This phenomenon has been observed for a wide variety of systems, including solutions of DNA [1,2], F-actin [3–6], and polystyrene sulfonate [7]. For flexible chains, polyvalent counterions can induce collapse of the chains into a globular compact structure [7]; alternatively, one can argue that the flexible chains mediate attractions between polyvalent counterions that cause them to aggregate. For rigid rods, on the other hand, the polyvalent counterions always repel each other along the axis of the rods, and the attraction between rods is attributed to ion-ion correlations among rods [8,9].

In this paper, we study the intermediate case of semiflexible chains, appropriate to biologically important polymers such as DNA. It has been shown theoretically that counterion correlations can modify the bending rigidity of a single semiflexible chain [10–12] and can even render the chain unstable to collapse [11]. Here, we consider two semiflexible chains from a different point of view: instead of studying how counterions modify the effective interactions between monomers on chains, we examine how chain flexibility modifies the effective interaction between generalized *linkers,* which could be simple polyvalent counterions [6] or weakly binding (cross-linking or bundling) proteins [4]. Alternatively, the linkers could represent hydrogen bonds connecting the two strands of a DNA double helix undergoing denaturation [13,14]. We use this effective interaction to study the many-body statistical mechanics of linkers. A similar approach has been fruitful for understanding behavior of proteins that link together elastic membranes [15,16].

Our calculations yield three main results. First, we find that the chain-mediated interactions between linkers are nonmonotonic. At large linker separations the chain bending elasticity leads to a long-ranged repulsion, while at short distances the electrostatic repulsion between chains leads to a short-ranged attraction between linkers. Consequently, there is a repulsive barrier in the interaction between two linkers at intermediate separations. Second, the unusual shape of the effective potential leads to interesting phase behavior in the many-linker system. Since the two-chain system is one dimensional, there is no true phase transition [17]; instead, we find a rounded transition from a dilute phase of linkers where the chains form large loops to a dense one where the chains are parallel and close together. The rounded transition is accompanied by large fluctuations in the spacing of linkers. This is reminiscent of large fluctuations in the separation of membranes near their binding/unbinding transition [18]. Third, we find that the onset of aggregation of single chains into pairs occurs within this rounded transition. Our results suggest that in many-chain systems, the rounded transition might be found near the onset of bundling.

Our model consists of two charged semiflexible chains held together by a series of linkers (Fig. 1). Each chain

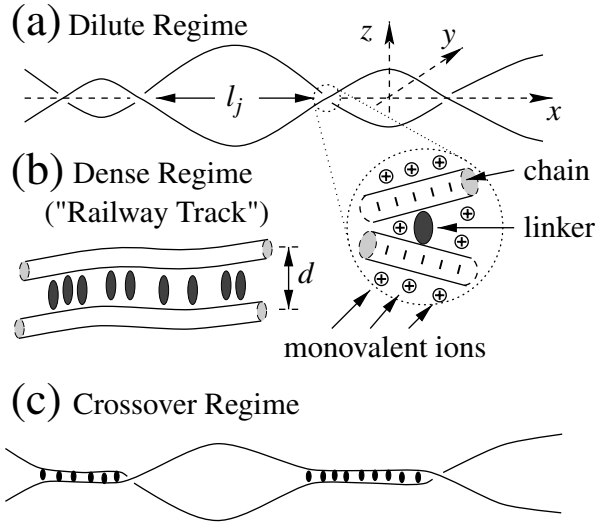

FIG. 1. Schematic view of two chains connected by linkers at (a) low linker densities (the dilute regime); (b) high densities (the disordered "railway track" structure), and (c) intermediate densities (the crossover regime). One chain is in the $y = 0$ plane, while the other is in the $y = d$ plane.

 0031-9007/01/86(10)/2182(4)$15.00

carries a negative linear charge density $\lambda = -e\xi/l_B$, where e is the electronic charge, $l_B = e^2/\varepsilon k_B T$ is the Bjerrum length, ε is the solution dielectric constant, and $k_B T$ is the thermal energy. Here, λ and ξ are the effective linear charge density and the corresponding, dimensionless, Manning-Oosawa parameter [8,19], respectively. In the presence of salt at concentration c_b, the Debye-Hückel screening length $\kappa^{-1} = 1/\sqrt{8\pi l_B c_b}$ characterizes the exponential decay of electrostatic interactions. We assume that a linker of size b constrains the two chains of radius r_s at a fixed separation $d = 2r_s + b$.

The first step is to calculate the effective interaction between two linkers separated by a distance l. This energy can be estimated by considering the total energy of a periodic array of linkers with separation distance l along the x axis. For simplicity, we assume that each chain is restricted to a plane parallel to the xz plane. One chain is located in the $y = 0$ plane and follows the curve $\{x, y, z\} = \{x, 0, z(x)\}$, where $z(\pm l/2) = 0$ and $z(0) = h/2$. The second chain is located in the $y = d$ plane and follows the curve $\{x, y, z\} = \{x, d, -z(x)\}$. A periodic trial function is assumed for the two chains

$$z(x) = \frac{h}{2}\cos(\pi x/l)\,, \tag{1}$$

where h is related to the cross-link angle θ through $\tan(\theta/2) = \pi h/2l$ and will be determined variationally. It should be emphasized that although the exact shape of the trial function affects the numerical values, it should not have a qualitative effect on the results.

The electrostatic energy per linker is given by

$$E_{\rm el} = \frac{\xi^2}{l_B}\int_{-l/2}^{l/2} dx\,(1 + z_x^2)^{1/2} \times \int_{\infty}^{\infty} dx'(1 + z_{x'}^2)^{1/2}\frac{e^{-\kappa r_{12}}}{r_{12}}\,, \tag{2}$$

where $r_{12}^2 = (x - x')^2 + d^2 + [z(x) + z(x')]^2$ and $z_x \equiv dz/dx$. In Eq. (2) and in the following discussion all energies are expressed in terms of the thermal energy $k_B T$. Note that if two straight chains cross at an angle θ, the electrostatic energy is [19]

$$E_{\rm el} = \frac{2\pi\xi^2 e^{-\kappa d}}{\kappa l_B \sin\theta} \equiv \frac{\Gamma}{\sin\theta} \tag{3}$$

favoring a crossing angle of $\theta = 90°$ and providing a basic energy scale in the problem.

This interaction competes with the bending energy [20]

$$E_{\rm bend} = l_p\int_{-l/2}^{l/2} dx\,(1 + z_x^2)^{-5/2} z_{xx}^2\,, \tag{4}$$

which favors small crossing angles. The chain persistence length l_p characterizes the decay of correlations in the chain orientation. Any dependence of bending rigidity on the composition of the surrounding solution [10–12,21] is implicit in l_p.

The total free energy per linker $f(l; h) = E_{\rm el} + E_{\rm bend}$ can be calculated numerically and minimized with respect to h [22]. Typical interaction energies $\Delta f(l) \equiv f(l) - f(\infty)$, as well as the behavior of the crossing angle θ, are depicted in Fig. 2. Note that $f(l \to \infty) = \Gamma$.

The competition between interchain electrostatic repulsion and intrachain bending rigidity leads to an effective attraction between linkers at short separations and an effective repulsion between linkers at large separations. At short separations, the bending energy dominates over the electrostatic energy and the chains remain parallel to each other (crossing angle $\theta = 0$). Since the chains are straight, the bending energy does not otherwise affect the linker interaction. Furthermore, the total electrostatic repulsion between chains is fixed and does not depend on the position of the linkers. As the density of linkers increases, the energy per linker decreases. The effective interaction can be estimated from the electrostatic energy of two parallel chains [19]. It is attractive and depends linearly on the linker separation: $\Delta f_{\rm short} \simeq -\Gamma(l_0 - l)/l_0$, where $\kappa l_0 = \pi/e^{\kappa d}K_0(\kappa d)$ and K_0 is the zero-order modified Bessel function. The origin of the attraction can also be understood by considering only two linkers: by joining to form a single junction instead of two separate junctions, the electrostatic repulsion between the chains is reduced by roughly the junction energy Γ. Thus, the interchain *repulsion* leads to an effective interlinker *attraction*.

At very large interlinker separations, the electrostatic repulsion dominates the bending energy and the crossing

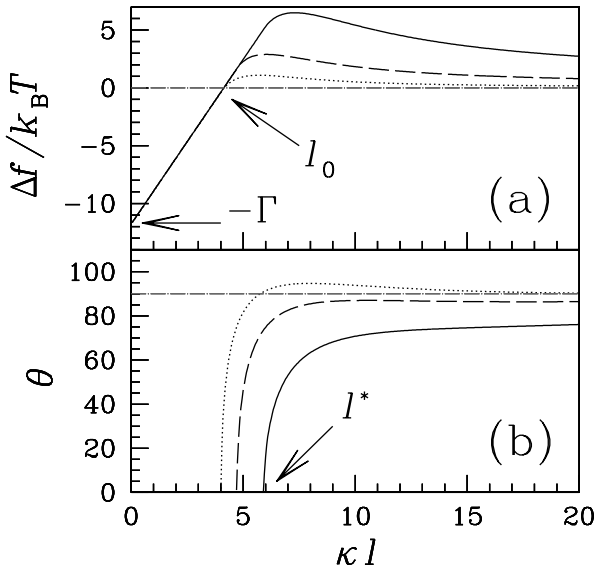

FIG. 2. (a) Interaction free energy per cross-link $\Delta f(l) = f(l) - \Gamma$ and (b) crossing angle θ as functions of the reduced distance κl between linkers. Note that $\Delta f(l)$ changes sign near l_0 (see text) and that θ becomes nonzero at l^* (denoted by an arrow for the solid curve). The curves correspond to different values of the chain persistence length $l_p = 10$ Å (dots), $l_p = 50$ Å (long dashes), and $l_p = 200$ Å (solid curve). We use $d = 25$ Å, $\xi = 4$, $\kappa^{-1} = 10$ Å, and $l_B = 7$ Å.

angles saturate to $\theta = 90°$. Since the chains are perpendicular at the junctions, the electrostatic repulsion does not otherwise affect the interaction between linkers. Compressing the linkers together costs bending energy, leading to a long-range repulsion of the form $\Delta f_{\text{long}} \simeq \alpha l_p/l$, where α is a constant of order unity. We estimate $\alpha \simeq \pi/\sqrt{2}$ by assuming constant curvature of the two chains in between junctions and minimizing with respect to θ. The crossover between the two regimes occurs at a separation l^*, where $|\Delta f_{\text{long}}| \simeq |\Delta f_{\text{short}}|$. For $l_p \lesssim \Gamma l_0$ (as is the case for the parameters in Fig. 2) we obtain $l^* \simeq l_0 + \alpha l_p/\Gamma$. For stiffer chains, we find $l^* \approx \sqrt{\alpha l_p l_0/\Gamma}$.

The final interlinker potential we use is

$$v(l) = \Delta f(l) + c \ln(l/l_p), \tag{5}$$

where the second term estimates the entropy loss of two random walks of step size l_p constrained to cross after the same number of steps at a distance l from each other [13]. We use $c = 3/2$ which corresponds to ideal chains in three dimensions. A recent estimate which includes excluded volume interactions between different parts of the chains yields $c \simeq 2.1$–2.2 [14]. This term is relevant only at large distances $l \gg l_p$. In addition, the linker size b provides a lower cutoff on the interlinker separation l. This corresponds to a hard-core repulsion or, in the case of DNA denaturation, to the size of one base pair. Other direct interactions between linkers such as the Coulomb repulsion between polyvalent counterions can also be included [22] but do not affect our main results.

With the effective linker interaction now in hand, we can study a one-dimensional fluid of N interacting linkers located along a straight line of length L at $0 \le x_1 < x_2 < \cdots < x_N \le L$. At low densities (large separations between linkers) one might expect a crystal of linkers even in this one-dimensional system because the effective repulsion decays as $1/l$. However, in this regime, the crossing angle is $\theta = 90°$ and the chain configuration on one side of the crossing junction is decoupled from the chain configuration on the other side. As a result, the linker interaction is only a nearest neighbor interaction; that is, the interaction decays as $1/l$, but only as far as the nearest linker.

For nearest neighbor interactions, one can calculate the partition function directly from the interlinker potential $v(l_j \equiv x_{j+1} - x_j)$. Note that at higher densities, the crossing angle becomes less than $\theta = 90°$ and further-neighbor interactions develop. Nevertheless, at those shorter separations, the interaction no longer has the form $1/l$, so the further-neighbor interactions cannot lead to new phase transitions, although they might affect quantitative results. We therefore neglect further-neighbor interactions at all densities.

It is convenient to use the Gibbs ensemble in which the natural variables are the number of linkers N and the one-dimensional pressure P [23]. In the thermodynamic limit the Gibbs free energy is $G = -N \ln Z_1$, where

$$Z_1 = \int_b^\infty \frac{dl}{\lambda_T} \exp[-v(l) - Pl] \tag{6}$$

and λ_T is the thermal wavelength. The chemical potential is $\mu = -\ln Z_1$ and the linker density $\rho = N/L$ can be calculated from the average linker separation $1/\rho = \bar{l} = -\partial(\ln Z_1)/\partial P$. The fluctuations in the separations $\Delta l^2 \equiv \overline{(l - \bar{l})^2}$ can be similarly extracted.

The typical behavior we obtain is shown in Fig. 3, where we plot the linker density ρ as a function of chemical potential μ (shifted by $\Gamma - 2\varepsilon_0$, where ε_0 is the adsorption energy of a linker onto a chain). Note that adsorption energies and a constant Γ term are not included in the definition of μ. At low μ the linker density is low and the chains form large loops between the linkers (Fig. 1a). At high ρ, on the other hand, the system resembles a disordered railway track where the chains are rails and linkers are ties (Fig. 1b).

Between these two limits, we find that at a certain value of the chemical potential $\mu^* \lesssim -\Gamma$ the linkers aggregate together and the density jumps sharply. The slope at the jump appears vertical because $d\rho/d\mu$ is large. Within our model, there is no true phase transition [17]. However, this jump in ρ can be viewed as a rounded transition from a dilute to a dense phase of linkers. In the vicinity of the rounded transition there are large fluctuations in the interlinker separation, as shown in the inset in Fig. 3. These fluctuations correspond to clusters of linkers that increase in size as the system crosses through the rounded transition. The crossover regime is limited to a narrow region around μ^* but spreads over a considerable range of densities ($0 \lesssim \rho \lesssim 0.2$ in the figure). Finally, we find that

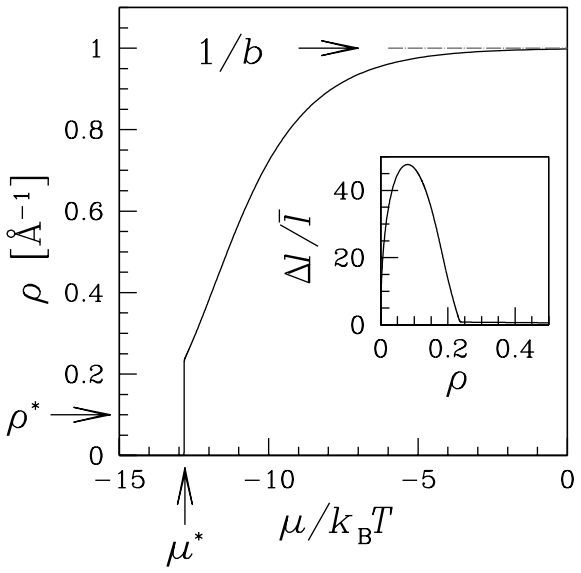

FIG. 3. One-dimensional linker density ρ as a function of the chemical potential μ and (inset) the relative fluctuation in the interlinker separation $\Delta l/\bar{l}$ as a function of ρ. The parameters are the same as for the solid curve in Fig. 2 for which $\Gamma \simeq 11.8$; also, $b = 1$ Å and $\lambda_T = 1$ Å.

as the density increases near the rounded transition, the short-ranged attraction between linkers sets in and the free energy drops rapidly. As a result, paired chains become favorable compared to isolated chains. Thus, the transition from single chains to pairs occurs near the rounded transition ($\mu \simeq \mu^*$). The density ρ^* at which chain pairing occurs can be estimated using analytical approximations for the different asymptotic regimes [22]. For the physical values used in Fig. 3 we find ρ^* to be well within the rounded transition.

Our simple model can also be applied to DNA melting [13,14], if the hydrogen bonds are considered to be generalized linkers. Existing models also show a sharp melting transition. The advantage of our approach is that some of the physical aspects of the chain interactions (namely, electrostatics and bending rigidity) are taken into account explicitly. On the other hand, the specific double helical structure of double stranded DNA is not included in the model. One straightforward generalization of the model would be to include a sequence-dependent linking energy reflecting the different number of hydrogen bonds connecting adenine with thymine and cytosine with guanine.

It is difficult to generalize our approach from two chains to many chains because many-body effects become important. Nevertheless, we expect our results to be reflected in the behavior of many-chain solutions. We note that the railway track structure resembles a bundle where the chains are parallel and the linker density is high [24]. Similarly, the dilute large-loop regime is reminiscent of networks where the chains cross at large angles and the linker density is low. Such structures have been observed experimentally [4,6]. Finally, in the limit of isolated chains the railway track is analogous to the compact torus formed in highly dilute DNA solutions [1,2,25].

We thank A. Ben-Shaul, K.-C. Lee, C. Marques, H. Schiessel, J.-L. Sikorav, M. Stevens, and J. Widom for valuable discussions. We also benefited from correspondence with B. Jancovici, J. L. Lebowitz, and H. Spohn. Support from NSF Grant No. DMR-9708646 and Israel–U.S. BSF Grant No. 97-00205 is gratefully acknowledged.

[1] V. A. Bloomfield, Biopolymers **31**, 1471 (1991); H. Deng and V. A. Bloomfield, Biophys. J. **77**, 1556 (1999).

[2] J. Pelta, F. Livolant, and J.-L. Sikorav, J. Biol. Chem. **271**, 5656 (1996); E. Raspaud, M. Olvera de la Cruz, J.-L. Sikorav, and F. Livolant, Biophys. J. **74**, 381 (1998); E. Raspaud, I. Chaperon, A. Leforestier, and F. Livolant, Biophys. J. **77**, 1547 (1999).

[3] M. Kawamura and K. Maruyama, J. Biochem. **68**, 899 (1970).

[4] T. D. Pollard and J. A. Cooper, Annu. Rev. Biochem. **55**, 987 (1986).

[5] J. X. Tang and P. A. Janmey, J. Biol. Chem. **271**, 8556 (1996); J. X. Tang, Sh. Wong, Ph. T. Tran, and P. A. Janmey, Ber. Bunsen.-Ges. Phys. Chem. **100**, 796 (1996).

[6] C. Safinya and G. Wong (private communication).

[7] M. Olvera de la Cruz, L. Belloni, M. Delsanti, J. P. Dalbiez, O. Spalla, and M. Drifford, J. Chem. Phys. **103**, 5781 (1995).

[8] F. Oosawa, *Polyelectrolytes* (Marcel Dekker, New York, 1971).

[9] J. Ray and G. S. Manning, Langmuir **10**, 2450 (1994); N. Grønbech-Jensen, R. J. Mashl, R. F. Bruinsma, and W. M. Gelbart, Phys. Rev. Lett. **78**, 2477 (1997); B.-Y. Ha and A. J. Liu, Phys. Rev. Lett. **79**, 1289 (1997); Phys. Rev. E **60**, 803 (1999); B. I. Shklovskii, Phys. Rev. Lett. **82**, 3268 (1999).

[10] I. Rouzina and V. A. Bloomfield, Biophys. J. **74**, 3152 (1998).

[11] R. Golestanian, M. Kardar, and T. B. Liverpool, Phys. Rev. Lett. **82**, 4456 (1999).

[12] H. Diamant and D. Andelman, Phys. Rev. E. **61**, 6740 (2000).

[13] See, e.g., D. Poland and H. A. Scheraga, *Theory of Helix-Coil Transitions in Biopolymers* (Academic Press, New York, 1970); M. Peyrard and A. R. Bishop, Phys. Rev. Lett. **62**, 2755 (1989); A. Yu. Grosberg and A. R. Khokhlov, *Statistical Physics of Macromolecules* (American Institute of Physics, New York, 1994), and references therein.

[14] Y. Kafri, D. Mukamel, and L. Peliti, Phys. Rev. Lett. **85**, 4988 (2000); see also T. Garel, C. Monthus, and H. Orland, e-print cond-mat/0101058.

[15] M. Goulian, R. Bruinsma, and P. Pincus, Europhys. Lett. **22**, 145 (1993); **23**, 155(E) (1993); R. Bruinsma and P. Pincus, Curr. Opin. Solid State Mater. Sci. **1**, 401 (1996).

[16] R. Menes and S. A. Safran, Phys. Rev. E **56**, 1891 (1997).

[17] The exact nature of the transition depends strongly on the interactions between different parts of the two-chain complex. It has been argued that excluded volume interactions can, in fact, induce a true first order phase transition [13,14]. This effect will not be taken into account in the current discussion.

[18] R. Lipowsky and S. Leibler, Phys. Rev. Lett. **56**, 2541 (1986); **59**, 1983(E) (1987); S. Leibler and R. Lipowsky, Phys. Rev. B **35**, 7004 (1987).

[19] S. L. Brenner and V. A. Parsegian, Biophys. J. **14**, 327 (1974).

[20] P. L. Hansen, D. Svenšek, V. A. Parsegian, and R. Podgornik, Phys. Rev. E **60**, 1956 (1999).

[21] T. Odijk, J. Polym. Sci. **15**, 477 (1977); J. Skolnick and M. Fixman, Macromolecules **10**, 944 (1977).

[22] I. Borukhov, R. F. Bruinsma, W. M. Gelbart, and A. J. Liu (to be published).

[23] See, e.g., E. H. Lieb and D. C. Mattis, *Mathematical Physics in One Dimension* (Academic Press, New York, 1966), and references therein.

[24] M. Stevens, Phys. Rev. Lett. **82**, 101 (1999).

[25] L. C. Gosule and J. C. Schellman, Science **259**, 333 (1976).